## Supplementary-Figures

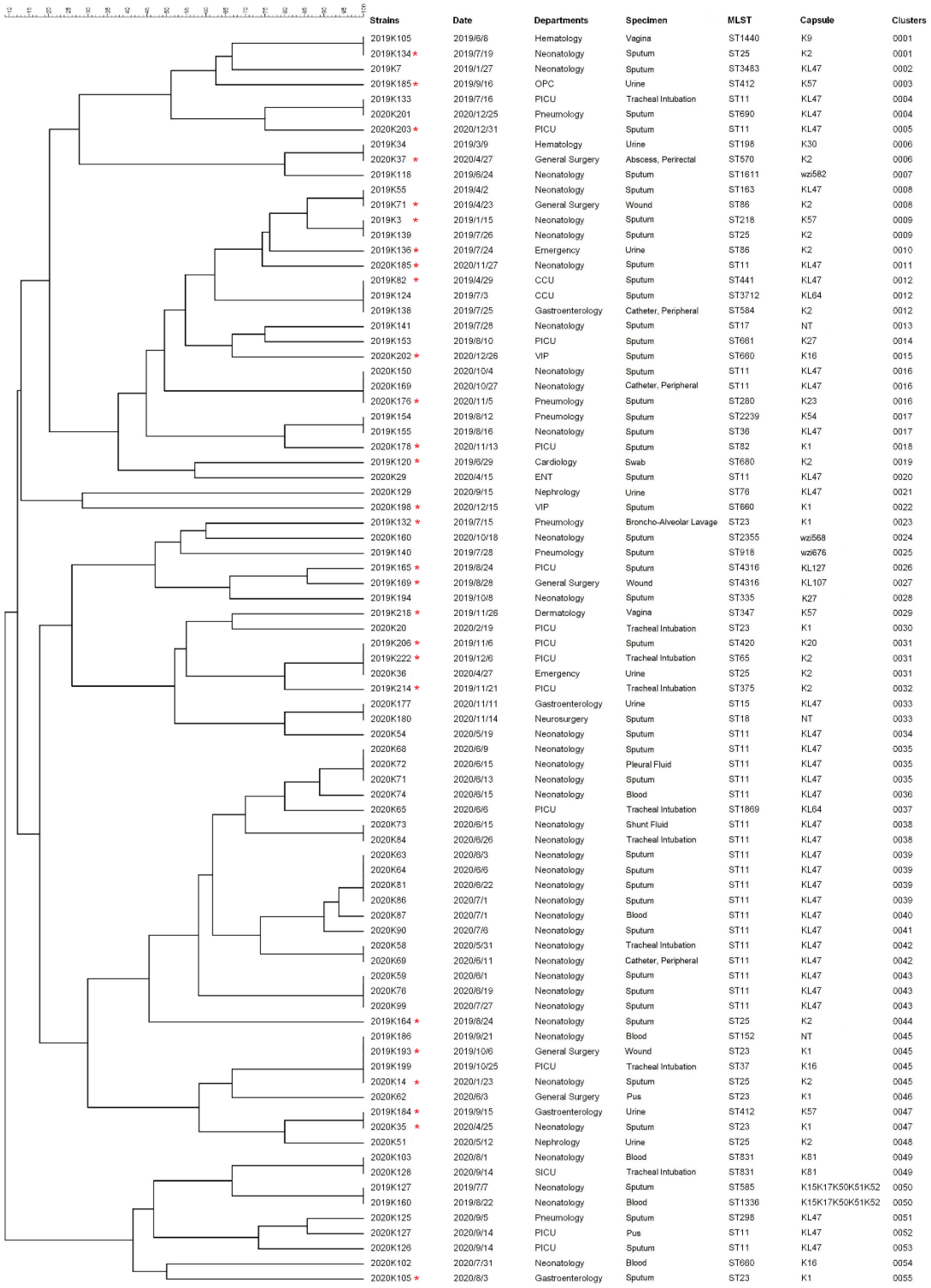

| Strains | Date | Departments | Specimen | MLST | Capsule | Clusters |
|---|---|---|---|---|---|---|
| 2019K105 | 2019/6/8 | Hematology | Vagina | ST1440 | K9 | 0001 |
| 2019K134 * | 2019/7/19 | Neonatology | Sputum | ST25 | K2 | 0001 |
| 2019K7 | 2019/1/27 | Neonatology | Sputum | ST3483 | KL47 | 0002 |
| 2019K185 * | 2019/9/16 | OPC | Urine | ST412 | K57 | 0003 |
| 2019K133 | 2019/7/16 | PICU | Tracheal Intubation | ST11 | KL47 | 0004 |
| 2020K201 | 2020/12/25 | Pneumology | Sputum | ST690 | KL47 | 0004 |
| 2020K203 * | 2020/12/31 | PICU | Sputum | ST11 | KL47 | 0005 |
| 2019K34 | 2019/3/9 | Hematology | Urine | ST198 | K30 | 0006 |
| 2020K37 * | 2020/4/27 | General Surgery | Abscess, Perirectal | ST570 | K2 | 0006 |
| 2019K118 | 2019/6/24 | Neonatology | Sputum | ST1611 | wzi582 | 0007 |
| 2019K55 | 2019/4/2 | Neonatology | Sputum | ST163 | KL47 | 0008 |
| 2019K71 * | 2019/4/23 | General Surgery | Wound | ST86 | K2 | 0008 |
| 2019K3 * | 2019/1/15 | Neonatology | Sputum | ST218 | K57 | 0009 |
| 2019K139 | 2019/7/26 | Neonatology | Sputum | ST25 | K2 | 0009 |
| 2019K136 * | 2019/7/24 | Emergency | Urine | ST86 | K2 | 0010 |
| 2020K185 * | 2020/11/27 | Neonatology | Sputum | ST11 | KL47 | 0011 |
| 2019K82 * | 2019/4/29 | CCU | Sputum | ST441 | KL47 | 0012 |
| 2019K124 | 2019/7/3 | CCU | Sputum | ST3712 | KL64 | 0012 |
| 2019K138 | 2019/7/25 | Gastroenterology | Catheter, Peripheral | ST584 | K2 | 0012 |
| 2019K141 | 2019/7/28 | Neonatology | Sputum | ST17 | NT | 0013 |
| 2019K153 | 2019/8/10 | PICU | Sputum | ST661 | K27 | 0014 |
| 2020K202 * | 2020/12/26 | VIP | Sputum | ST660 | K16 | 0015 |
| 2020K150 | 2020/10/4 | Neonatology | Sputum | ST11 | KL47 | 0016 |
| 2020K169 | 2020/10/27 | Neonatology | Catheter, Peripheral | ST11 | KL47 | 0016 |
| 2020K176 * | 2020/11/5 | Pneumology | Sputum | ST280 | K23 | 0016 |
| 2019K154 | 2019/8/12 | Pneumology | Sputum | ST2239 | K54 | 0017 |
| 2019K155 | 2019/8/16 | Neonatology | Sputum | ST36 | KL47 | 0017 |
| 2020K178 * | 2020/11/13 | PICU | Sputum | ST82 | K1 | 0018 |
| 2019K120 * | 2019/6/29 | Cardiology | Swab | ST680 | K2 | 0019 |
| 2020K29 | 2020/4/15 | ENT | Sputum | ST11 | KL47 | 0020 |
| 2020K129 | 2020/9/15 | Nephrology | Urine | ST76 | KL47 | 0021 |
| 2020K198 * | 2020/12/15 | VIP | Sputum | ST660 | K1 | 0022 |
| 2019K132 * | 2019/7/15 | Pneumology | Broncho-Alveolar Lavage | ST23 | K1 | 0023 |
| 2020K160 | 2020/10/18 | Neonatology | Sputum | ST2355 | wzi568 | 0024 |
| 2019K140 | 2019/7/28 | Pneumology | Sputum | ST918 | wzi676 | 0025 |
| 2019K165 * | 2019/8/24 | PICU | Sputum | ST4316 | KL127 | 0026 |
| 2019K169 * | 2019/8/28 | General Surgery | Wound | ST4316 | KL107 | 0027 |
| 2019K194 | 2019/10/8 | Neonatology | Sputum | ST335 | K27 | 0028 |
| 2019K218 * | 2019/11/26 | Dermatology | Vagina | ST347 | K57 | 0029 |
| 2020K20 | 2020/2/19 | PICU | Tracheal Intubation | ST23 | K1 | 0030 |
| 2019K206 * | 2019/11/6 | PICU | Sputum | ST420 | K20 | 0031 |
| 2019K222 * | 2019/12/6 | PICU | Tracheal Intubation | ST65 | K2 | 0031 |
| 2020K36 | 2020/4/27 | Emergency | Urine | ST25 | K2 | 0031 |
| 2019K214 * | 2019/11/21 | PICU | Tracheal Intubation | ST375 | K2 | 0032 |
| 2020K177 | 2020/11/11 | Gastroenterology | Urine | ST15 | KL47 | 0033 |
| 2020K180 | 2020/11/14 | Neurosurgery | Sputum | ST18 | NT | 0033 |
| 2020K54 | 2020/5/19 | Neonatology | Sputum | ST11 | KL47 | 0034 |
| 2020K68 | 2020/6/9 | Neonatology | Sputum | ST11 | KL47 | 0035 |
| 2020K72 | 2020/6/15 | Neonatology | Pleural Fluid | ST11 | KL47 | 0035 |
| 2020K71 | 2020/6/13 | Neonatology | Sputum | ST11 | KL47 | 0035 |
| 2020K74 | 2020/6/15 | Neonatology | Blood | ST11 | KL47 | 0036 |
| 2020K65 | 2020/6/6 | PICU | Tracheal Intubation | ST1869 | KL64 | 0037 |
| 2020K73 | 2020/6/15 | Neonatology | Shunt Fluid | ST11 | KL47 | 0038 |
| 2020K84 | 2020/6/26 | Neonatology | Tracheal Intubation | ST11 | KL47 | 0038 |
| 2020K63 | 2020/6/3 | Neonatology | Sputum | ST11 | KL47 | 0039 |
| 2020K64 | 2020/6/6 | Neonatology | Sputum | ST11 | KL47 | 0039 |
| 2020K81 | 2020/6/22 | Neonatology | Sputum | ST11 | KL47 | 0039 |
| 2020K86 | 2020/7/1 | Neonatology | Sputum | ST11 | KL47 | 0039 |
| 2020K87 | 2020/7/1 | Neonatology | Blood | ST11 | KL47 | 0040 |
| 2020K90 | 2020/7/6 | Neonatology | Sputum | ST11 | KL47 | 0041 |
| 2020K58 | 2020/5/31 | Neonatology | Tracheal Intubation | ST11 | KL47 | 0042 |
| 2020K69 | 2020/6/11 | Neonatology | Catheter, Peripheral | ST11 | KL47 | 0042 |
| 2020K59 | 2020/6/1 | Neonatology | Sputum | ST11 | KL47 | 0043 |
| 2020K76 | 2020/6/19 | Neonatology | Sputum | ST11 | KL47 | 0043 |
| 2020K99 | 2020/7/27 | Neonatology | Sputum | ST11 | KL47 | 0043 |
| 2019K164 * | 2019/8/24 | Neonatology | Sputum | ST25 | K2 | 0044 |
| 2019K186 | 2019/9/21 | Neonatology | Blood | ST152 | NT | 0045 |
| 2019K193 * | 2019/10/6 | General Surgery | Wound | ST23 | K1 | 0045 |
| 2019K199 | 2019/10/25 | PICU | Tracheal Intubation | ST37 | K16 | 0045 |
| 2020K14 * | 2020/1/23 | Neonatology | Sputum | ST25 | K2 | 0045 |
| 2020K62 | 2020/6/3 | General Surgery | Pus | ST23 | K1 | 0046 |
| 2019K184 * | 2019/9/15 | Gastroenterology | Urine | ST412 | K57 | 0047 |
| 2020K35 * | 2020/4/25 | Neonatology | Sputum | ST23 | K1 | 0047 |
| 2020K51 | 2020/5/12 | Nephrology | Urine | ST25 | K2 | 0048 |
| 2020K103 | 2020/8/1 | Neonatology | Blood | ST831 | K81 | 0049 |
| 2020K128 | 2020/9/14 | SICU | Tracheal Intubation | ST831 | K81 | 0049 |
| 2019K127 | 2019/7/7 | Neonatology | Sputum | ST585 | K15K17K50K51K52 | 0050 |
| 2019K160 | 2019/8/22 | Neonatology | Blood | ST1336 | K15K17K50K51K52 | 0050 |
| 2020K125 | 2020/9/5 | Pneumology | Sputum | ST298 | KL47 | 0051 |
| 2020K127 | 2020/9/14 | PICU | Pus | ST11 | KL47 | 0052 |
| 2020K126 | 2020/9/14 | PICU | Sputum | ST11 | KL47 | 0053 |
| 2020K102 | 2020/7/31 | Neonatology | Blood | ST660 | K16 | 0054 |
| 2020K105 * | 2020/8/3 | Gastroenterology | Sputum | ST23 | K1 | 0055 |

**FIGURE S1** Phylogenetic tree of hypervirulence genes positive *K. pneumoniae* (hgKp) isolates (n = 83). The evolutionary analysis for finger printing profiles of Intergenic Consensus-Polymerase Chain Reaction (ERIC-PCR) was performed by BioNumerics software. Strains marked red "*" were hypervirulent *K. pneumoniae.*

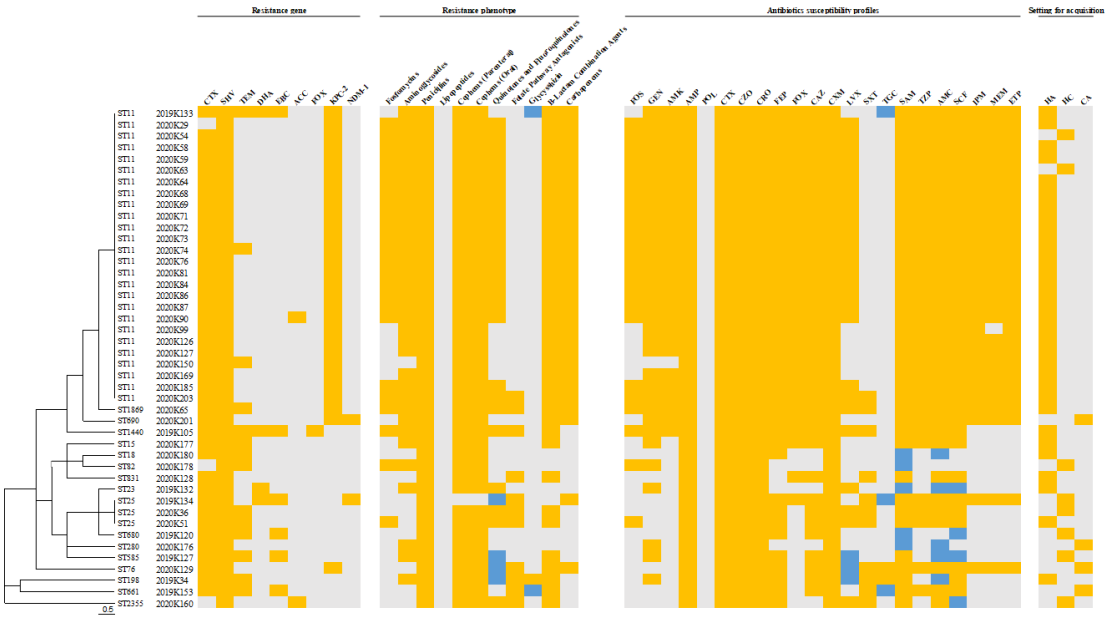


**FIGURE S2** Characteristics of MDR-hgKp isolates (n = 44). Resistance gene (left), predicted phenotype (middle), and antibiotics susceptibility profiles (right) of ESBLs-producing isolates (n = 44) (from top to bottom are isolates in the phylogenetic relationship analyzed by Phyloviz 2.0 software using the hierarchical clustering algorithm based on the complete-linkage method of hamming distance between STs). Yellow filling means resistant, blue means intermediate, and grey means susceptible. FOS, fosfomycin; GEN, gentamicin; AMK, amikacin; AMP, ampicillin; POL, polymyxin; CTX, cefotaxime; CZO, cefazolin; CRO, ceftriaxone; FEP, cefepime; FOX, cefoxitin; CAZ, ceftazidime; CXM, cefuroxime; LVX, levofloxacin; SXT, trimethoprim-sulfamethoxazole; TGC, tigecycline; SAM, ampicillin-sulbactam; TZP, piperacillin-tazobactam; AMC, amoxicillin-clavulanic acid; SCF, cefperazone-sulbactam; IPM, imipenem; MEM, meropenem; ETP, ertapenem; HA, hospital-associated infection; HC, healthcare- associated infection; CA, community- associated infection.

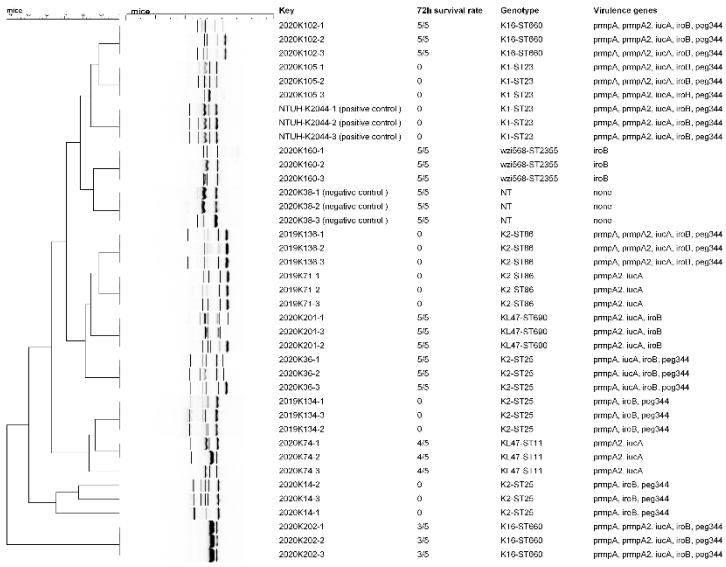


**FIGURE S3** Homology of randomly selected strains (n = 11) used to build murine sepsis model. Strains-1, strains before mice injection; Strains-2 and Strains-3, strains recovered from a separate portion of the harvested livers of the injected mice. Fresh livers were grinded in paraformaldehyde-free PBS. Bacteria in supernatant were cultured on blood agar plate at 37 ℃ overnight, and identified by MALDI-TOF mass spectrometry. The evolutionary analysis for finger printing profiles of Intergenic Consensus-Polymerase Chain Reaction (ERIC-PCR) was performed by BioNumerics software.

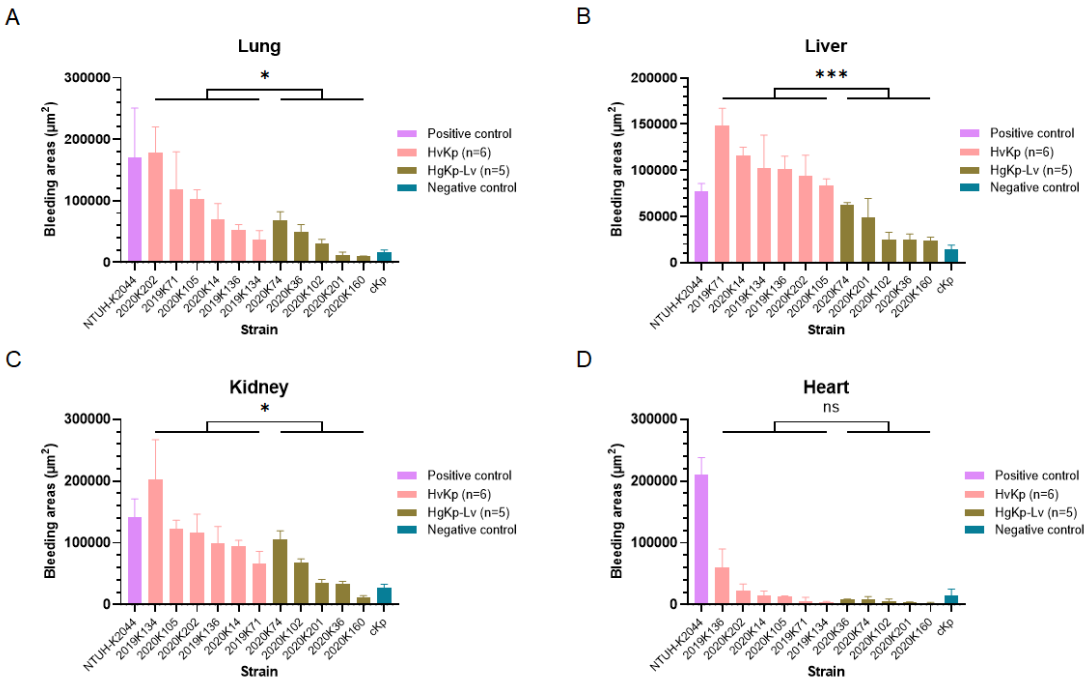


**FIGURE S4** Damage of hvKp infection to mice. Data of organs bleeding areas were expressed as means ± SDs, $P < 0.05$ (*), $P < 0.001$ (***) and $P > 0.05$ (ns). Between hvKp and hgKp-Lv isolates infected mice, significant differences were observed in the bleeding areas of lung (t = 2.33, $P = 0.0446$, 95% confidence interval [CI] = 42018 to 98612), of liver (t = 5.62, $P = 0.0003$, 95% CI = 1776.2 to 116974), of kidney (t = 2.58, $P = 0.0298$, 95% CI = 8126.2 to 124402), but not of heart (t = 1.66, $P = 0.1558$, 95% CI = -7219 to 35917) using independent-samples t-test.

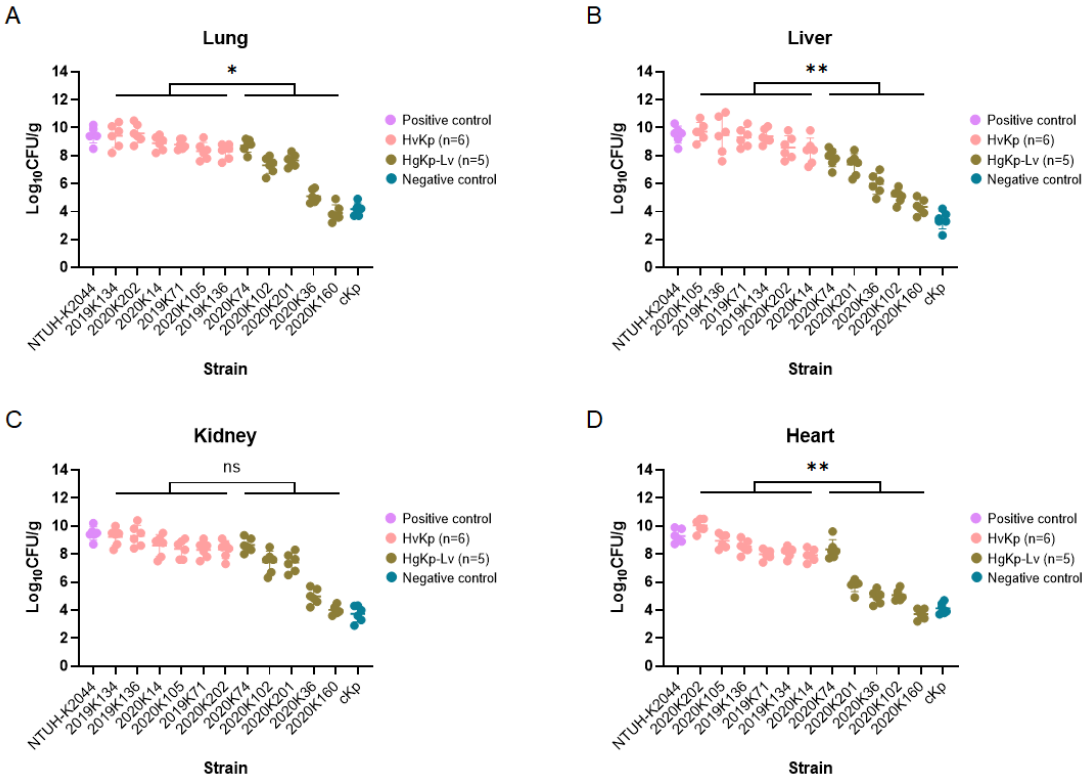


**FIGURE S5** Bacterial burdens in the mice organs. Data shown are means ± SDs, $P < 0.05$ (*), $P < 0.01$ (**) and $P > 0.05$ (ns). Between hvKp and hgKp-Lv isolates infected mice, significant differences were observed in bacterial CFU of lung (t = 2.81, $P = 0.0205$, 95% confidence interval [CI] = 6.6 to 9), of liver (t = 4.64, $P = 0.0012$, 95% CI = 6.5 to 9), of heart (t = 3.87, $P = 0.0038$, 95% CI = 5.9 to 8.5), and a slight difference was observed of kidney (t = 2.53, $P = 0.0596$, 95% CI = 6.5 to 8.8) using independent-samples t-test.